

# Therapeutic potential of clinical-grade human induced pluripotent stem cell-derived cardiac tissues



Hiroaki Osada, MD, PhD,<sup>a,b</sup> Masahide Kawatou, MD, PhD,<sup>a,b</sup> Daiki Fujita, MS,<sup>c</sup> Yasuhiko Tabata, PhD, DMedSci, DPharm,<sup>d</sup> Kenji Minatoya, MD, PhD,<sup>a</sup> Jun K. Yamashita, MD, PhD,<sup>b</sup> and Hidetoshi Masumoto, MD, PhD<sup>a,e</sup>

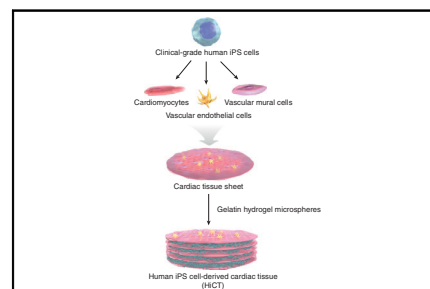
## ABSTRACT

**Objectives:** To establish a protocol to prepare and transplant clinical-grade human induced pluripotent stem cell (hiPSC)-derived cardiac tissues (HiCTs) and to evaluate the therapeutic potential in an animal myocardial infarction (MI) model.

**Methods:** We simultaneously differentiated clinical-grade hiPSCs into cardiovascular cell lineages with or without the administration of canonical Wnt inhibitors, generated 5-layer cell sheets with insertion of gelatin hydrogel microspheres (GHMs) (HiCTs), and transplanted them onto an athymic rat MI model. Cardiac function was evaluated by echocardiography and cardiac magnetic resonance imaging and compared with that in animals with sham and transplantation of 5-layer cell sheets without GHMs. Graft survival, ventricular remodeling, and neovascularization were evaluated histopathologically.

**Results:** The administration of Wnt inhibitors significantly promoted cardiomyocyte (CM) ( $P < .0001$ ) and vascular endothelial cell (EC) ( $P = .006$ ) induction, which resulted in cellular components of  $52.0 \pm 6.1\%$  CMs and  $9.9 \pm 3.0\%$  ECs. Functional analyses revealed the significantly lowest left ventricular end-diastolic volume and highest ejection fraction in the HiCT group. Histopathologic evaluation revealed that the HiCT group had a significantly larger median engrafted area (4 weeks, GHM(-) vs HiCT:  $0.4$  [range,  $0.2$ - $0.7$ ]  $\text{mm}^2$  vs  $2.2$  [range,  $1.8$ - $3.1$ ]  $\text{mm}^2$ ;  $P = .005$ ; 12 weeks,  $0$  [range,  $0$ - $0.2$ ]  $\text{mm}^2$  vs  $1.9$  [range,  $0.1$ - $3.2$ ]  $\text{mm}^2$ ;  $P = .026$ ), accompanied by the smallest scar area and highest vascular density at the MI border zone.

**Conclusions:** Transplantation of HiCTs generated from clinical-grade hiPSCs exhibited a prominent therapeutic potential in a rat MI model and may provide a promising therapeutic strategy in cardiac regenerative medicine. (JTCVS Open 2021;8:359-74)



HiCTs generated from clinical-grade hiPSCs show prominent therapeutic potential.

## CENTRAL MESSAGE

Transplantation of clinical-grade human induced pluripotent stem cell-derived cardiac tissues resulted in functional recovery in an animal myocardial infarction model and may be a promising therapeutic strategy in cardiac regenerative medicine.

## PERSPECTIVE

We have established a method to generate and transplant clinical-grade human induced pluripotent stem cell-derived cardiac tissues and validated their therapeutic potential in myocardial regeneration accompanied by vascular networks in an animal myocardial infarction model. The pre-clinical proof-of-concept of the efficacy of this therapeutic strategy provides further support for this therapeutic modality in patients with severe heart failure.

See Commentaries on pages 375 and 377.

From the <sup>a</sup>Department of Cardiovascular Surgery, Graduate School of Medicine, <sup>b</sup>Department of Cell Growth and Differentiation, Center for iPS Cell Research and Application, and <sup>d</sup>Department of Biomaterials, Institute for Frontier Life and Medical Sciences, Kyoto University, Kyoto, Japan; <sup>c</sup>iHeart Japan Corporation, Kyoto, Japan; and <sup>e</sup>Clinical Translational Research Program, RIKEN Center for Biosystems Dynamics Research, Kobe, Japan.

Support was provided by the Japan Agency for Medical Research and Development (Grant JP18he0702246, to H.M., Y.T., J.K.Y., and K.M.) and an Invited Research Project of the Institute for Advancement of Clinical Transnational Science, Kyoto University Hospital (to K.M.).

Received for publication April 21, 2021; accepted for publication Sept 24, 2021; available ahead of print Oct 15, 2021.

Address for reprints: Hidetoshi Masumoto, MD, PhD, Department of Cardiovascular Surgery, Graduate School of Medicine, Kyoto University, 54 Shogoin-Kawaharacho, Sakyo-ku, Kyoto 606-8507, Japan (E-mail: [masumoto@kuhp.kyoto-u.ac.jp](mailto:masumoto@kuhp.kyoto-u.ac.jp)); or Jun K. Yamashita, MD, PhD, Department of Cell Growth and Differentiation, Center for iPS Cell Research and Application, Kyoto University, 53 Shogoin-Kawaharacho, Sakyo-ku, Kyoto 606-8507, Japan (E-mail: [juny@cira.kyoto-u.ac.jp](mailto:juny@cira.kyoto-u.ac.jp)).


2666-2736

Copyright © 2021 The Author(s). Published by Elsevier Inc. on behalf of The American Association for Thoracic Surgery. This is an open access article under the CC BY-NC-ND license (<http://creativecommons.org/licenses/by-nc-nd/4.0/>).

<https://doi.org/10.1016/j.jtc.2021.09.038>

**Abbreviations and Acronyms**

3D	= 3-dimensional
$\alpha$ MEM	= alpha minimum essential medium
CM	= cardiomyocyte
cTnT	= cardiac isoform of troponin T
CUBIC	= clear, unobstructed brain imaging cocktails and computational analysis sample
EC	= endothelial cell
ESC	= embryonic stem cell
FBS	= fetal bovine serum
FS	= fractional shortening
GHM	= gelatin hydrogel microsphere
GMP	= good manufacturing protocol
HiCT	= human induced pluripotent stem cell–derived cardiac tissue
hiPSC	= human induced pluripotent stem cell
HLA	= human leukocyte antigen
iPSC	= induced pluripotent stem cell
LSFM	= light sheet fluorescence microscopy
LV	= left ventricular
LVDd	= left ventricular end-diastolic dimension
LVDs	= left ventricular end-systolic dimension
LVEDV	= left ventricular end-diastolic volume
LVEF	= left ventricular ejection fraction
MC	= mural cell
MI	= myocardial infarction
SD	= standard deviation
vWF	= von Willebrand factor

 Video clip is available online.

Stem cell products manufactured from various stem cell populations are being increasingly applied for cardiac regenerative therapy<sup>1-3</sup>. Among the stem cell populations tested in basic research, pluripotent stem cells, such as embryonic stem cells (ESCs) and induced pluripotent stem cells (iPSCs), have demonstrated a robust potential for cardiac function restoration owing to their ability to produce cardiovascular cells for supplementation to an injured heart.<sup>4</sup> Pluripotent stem cell–based cardiac regenerative therapy may be an optimal therapeutic strategy for severe heart failure, considering the shortage of donor hearts for organ transplantation worldwide.<sup>5,6</sup>

The benefit of iPSCs over ESCs is the availability of patients' own autologous cells for treatment. When iPSC products are generated autologously, better engraftment

free from the risk of immune rejection after transplantation can be theoretically anticipated. Despite the advantage of autologous iPSCs, disadvantages in the setting of autologous iPSC transplantation exist, including the cost and time required for quality control for each individual.<sup>7</sup> Furthermore, autologous cell products from patients with cardiomyopathy attributed to genetic mutations may take over its disease phenotype, which would hamper the therapeutic effects of the products. Clinical-grade human iPSCs (hiPSCs) established from human leukocyte antigen (HLA)-homozygous healthy volunteers are currently being considered as a quality-controlled cell source available for allogeneic transplantation. This cell stock or bank has been established in which good manufacturing protocol (GMP)-grade cell-processing facilities provide quality-controlled hiPSCs for clinical use.<sup>8-11</sup>

We have been investigating the systematic induction of various cardiovascular cells—cardiomyocytes (CMs), vascular endothelial cells (ECs), and vascular mural cells (MCs)—from ESCs and iPSCs and preclinical validation of the therapeutic potential of induced cardiovascular cell–engineered 3-dimensional (3D) transplantable grafts using animal disease models.<sup>12-18</sup>

In the present study, we aimed to evaluate the differentiation efficacy of clinical-grade hiPSCs into cardiovascular lineages as a cellular candidate for future clinical use and to validate the preclinical functional efficacy of transplantation surgery using hiPSC-derived cardiac tissue (HiCT) bioengineered by clinical-grade hiPSC-derived cardiac cell sheets and gelatin hydrogel microspheres (GHMs)<sup>19,20</sup> in a rat myocardial infarction (MI) model.

**METHODS**

The experimental materials and methods are described in more detail in [Appendix 1](#).

**Differentiation of Clinical-Grade hiPSCs Into Cardiovascular Cell Lineages**

We used clinical-grade hiPSC lines (Ffi01s04 and QHJ101s04) that are peripheral monocyte-derived HLA-homozygous hiPSCs established at the Facility for iPS Cell Therapy Center for iPS Cell Research and Application, Kyoto University, Japan. Clinical-grade hiPSCs were simultaneously differentiated into cardiovascular cell lineages with (Wi+) or without (Wi-) canonical Wnt inhibitors XAV939 and IWP4 at differentiation days 5 to 7 ([Figure 1, A](#)). At 13 to 15 days after differentiation, cardiovascular cells were dissociated and subjected to flow cytometry analysis. Cells from the Wi+ group were seeded onto 12-well temperature-responsive culture plates. At 2 to 4 days after seeding, self-pulsating cell sheets were collected and then subjected to flow cytometry analysis.

**Preparation of HiCTs**

We generated 5 layers of cell sheets with insertion of GHMs (HiCTs) and also prepared 5 layers of stacked sheets without GHMs [GHM(-)] for transplantation experiments.

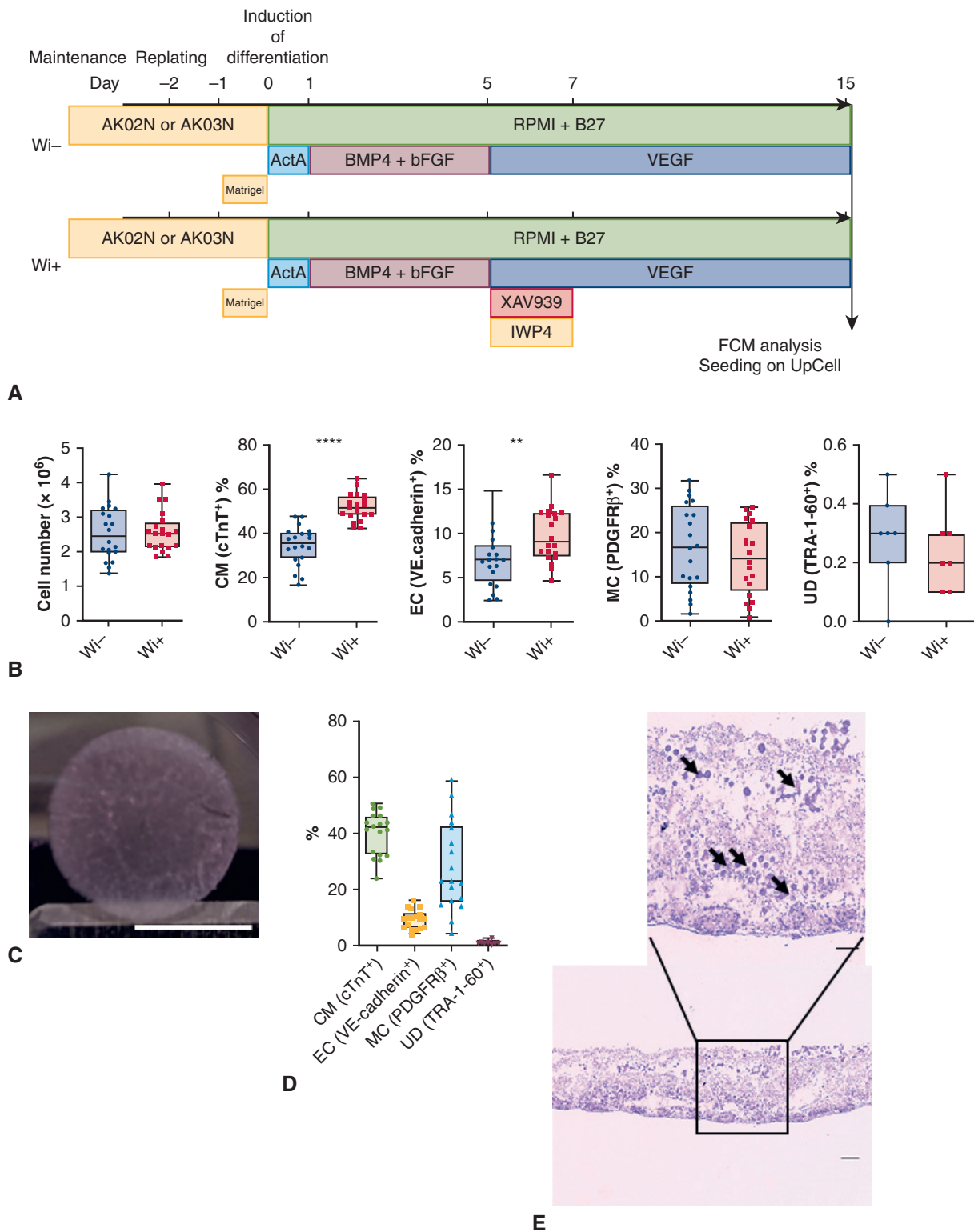


**FIGURE 1.** Differentiation of human induced pluripotent stem cells (hiPSCs) into cardiovascular cells and formation of human induced pluripotent stem cell–derived cardiac tissue (HiCT). **A**, Schematic of the induction protocol of clinical-grade hiPSCs into cardiovascular lineage cells with (Wi+) or without (Wi-) canonical Wnt inhibitors XAV939/IWP4 at differentiation day 5 to 7. *ActA*, activin A; *BMP4*, bone morphogenetic protein 4; *bFGF*, basic fibroblast growth factor; *VEGF*, vascular endothelial cell growth factor; *FCM*, flow cytometry. **B**, Cell number and cellular components of each population after differentiation. *CM*, cardiomyocyte; *EC*, vascular endothelial cell; *MC*, vascular mural cell; *UD*, undifferentiated cell, *cTnT*, cardiac isoform of troponin-T;

## Animals

Male athymic nude rats (F344/NJcl-mu/rnu, 8-12 weeks old) were purchased from CLEA Japan (Tokyo, Japan), and housed in a controlled environment. All animal experiment protocols were approved by the Animal Experimentation Committee of Kyoto University (#Med Kyo 19540). All animal experiments were performed according to the Guidelines for Animal Experiments of Kyoto University, which conform to Japanese law and the US National Research Council's *Guide for the Care and Use of Laboratory Animals*.

## Induction of MI, HiCT Transplantation, and Follow-up

MI was induced by permanent ligation of the left anterior descending coronary artery as reported previously.<sup>15</sup> Rats with left ventricular (LV) fractional shortening (FS) <30% by echocardiography on day 7 after ligation were enrolled in further experiments. Each enrolled rat was assigned at random to 1 of the 3 groups: 4-week observation, MI operation without transplantation group (sham; n = 18), 5-layer cell sheets without GHM transplantation group [GHM(-); n = 12], and the HiCT transplantation group (HiCT; n = 12). Parts of each group [sham, n = 8; GHM(-), n = 6; HiCT, n = 5] were followed up to 12 weeks post-transplantation. Echocardiography and cardiac magnetic resonance imaging (MRI) were conducted and compared among the groups.

At the end of the observation period, the animals were sacrificed, and graft survival, ventricular remodeling, and neovascularization after MI were histopathologically evaluated and compared among the groups. As a 3D evaluation of the vascular network formation among engrafted HiCTs, we performed light sheet fluorescence microscopy (LSFM) on transplanted rat hearts after tissue clearing by the clear, unobstructed brain imaging cocktails and computational analysis sample (CUBIC) method.<sup>21,22</sup>

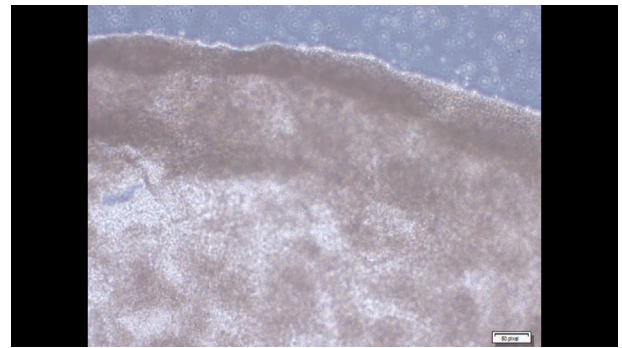
## Statistical Analysis

Nonnormally distributed data are presented as median (interquartile range [IQR]), and normally distributed data are presented as mean  $\pm$  standard deviation (SD). All data analyses were performed using JMP Pro 15.1 (SAS Institute, Cary, NC). *P* values for comparisons between 2 groups were obtained using the Wilcoxon/Kruskal–Wallis test. Comparisons between >2 groups were also performed using the Wilcoxon/Kruskal–Wallis test and post hoc comparisons between groups were performed with the Steel–Dwass multiple-comparison test. *P* < .05 was considered statistically significant.

## RESULTS

### Cardiovascular Cell Induction and Transplantable Cardiac Tissue Formation From Clinical-Grade hiPSCs

We collected cells on differentiation day 15 and subjected to flow cytometry for analysis of cellular components that resulted in significantly higher cardiac isoform of troponin



**VIDEO 1.** Representative movie of a self-pulsating cell sheet consisting of cardiovascular cells. Video available at: [https://www.jtcvs.org/article/S2666-2736\(21\)00340-5/fulltext](https://www.jtcvs.org/article/S2666-2736(21)00340-5/fulltext).

T (cTnT)<sup>+</sup> CM components (Wi- vs Wi+, 34.5  $\pm$  8.9% vs 52.0  $\pm$  6.1%; *P* < .0001) and VE-cadherin<sup>+</sup> EC components (Wi- vs Wi+, 7.1  $\pm$  3.1% vs 9.9  $\pm$  3.0%; *P* = .006) in the Wi + group. The total number of collected cells (Wi- vs Wi+, 2.5  $\pm$  0.8  $\times$  10<sup>6</sup> vs 2.6  $\pm$  0.6  $\times$  10<sup>6</sup>), PDGFR $\beta$ <sup>+</sup> MC component (Wi- vs Wi+, 16.7  $\pm$  9.6% vs 14.1  $\pm$  8.2%), and TRA-1-60<sup>+</sup> undifferentiated cell (UD) component (Wi- vs Wi+, 0.3  $\pm$  0.2% vs 0.2  $\pm$  0.1%) were not affected by the Wnt inhibitor treatment (Figure 1, B).

After 2 to 4 days of culture of cardiovascular cells from Wi + group cells, we collected self-pulsating cell sheets (Figure 1, C; Video 1) including 39.9  $\pm$  7.4% of cTnT<sup>+</sup> CMs, 9.3  $\pm$  3.2% of VE-cadherin<sup>+</sup> ECs, 26.4  $\pm$  16.1% of PDGFR $\beta$ <sup>+</sup> MCs, and 0.7% (IQR, 0.6%-1.0%) of TRA-1-60<sup>+</sup> UD (Figure 1, D). We layered the collected cell sheets using GHMs to generate HiCTs (Figure 1, E). The HiCT diameter was approximately 10 mm, and the thickness was approximately 800  $\mu$ m.

### Transplantation of HiCTs and Functional Recovery in a Rat MI Model

There were no significant differences among the 3 groups in echocardiographic parameters before transplantation (after MI induction). Echocardiography at 4 weeks post-transplantation revealed significantly lower LV diastolic dimension (LVDD) and LV end-diastolic volume (LVEDV) and higher LV ejection fraction (LVEF) and LV FS in the

VE-cadherin, vascular endothelial-cadherin, PDGFR $\beta$ , platelet-derived growth factor receptor beta. The addition of XAV939 and IWP4 clearly promoted an increase in CMs and ECs. The upper and lower borders of the box represent the upper and lower quartiles, and the middle horizontal line represents the median. The upper and lower whiskers represent the maximum and minimum values. \*\**P* < .01; \*\*\*\**P* < .0001, Wilcoxon/Kruskal–Wallis test (n = 20). C, Representative macroscopic view of the collected cell sheet on a temperature-responsive culture dish (UpCell). (Scale bar: 10 mm.) D, Cellular compositions of the collected cell sheet (n = 20). E, Representative hematoxylin and eosin staining of HiCT (maintained for 1 week in culture). The black arrows indicate gelatin hydrogel microspheres. (Scale bars: 100  $\mu$ m [upper]; 200  $\mu$ m [lower].)

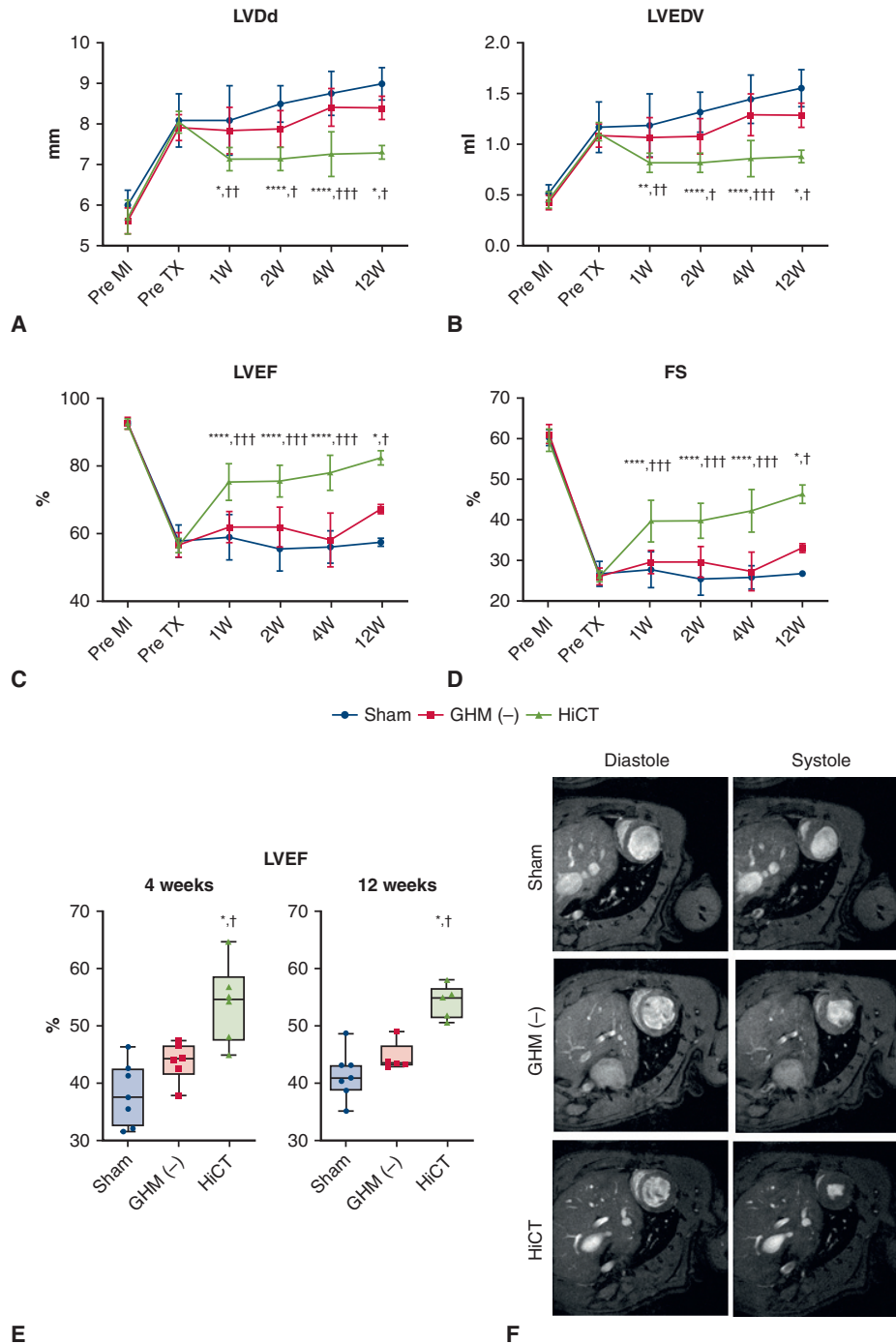


**FIGURE 2.** Cardiac function evaluation after human induced pluripotent stem cell–derived cardiac tissue (*HiCT*) transplantation. A–D, Echocardiography data over time post-transplantation: left ventricular (LV) end-diastolic dimension (*LVDD*) (A), LV end-diastolic volume (*LVEDV*) (B), LV ejection fraction (*LVEF*) (C), and LV fractional shortening (*FS*) (D). Echocardiography revealed significantly superior results in the *HiCT* group compared with other groups after transplantation. Data in the graphs are mean ± SD. \**P* < .05, \*\**P* < .01, \*\*\*\**P* < .0001 versus sham; †*P* < .05, ††*P* < .01, †††*P* < .001 versus gelatin hydrogel microsphere–negative [*GHM*(–)], Wilcoxon/Kruskal–Wallis test, post hoc Steel–Dwass multiple comparison test. Four-week observation: sham, *n* = 18; *GHM*(–), *n* = 12; *HiCT*, *n* = 12; 12-week observation: sham, *n* = 8; *GHM*(–), *n* = 6; *HiCT*, *n* = 5. E, Results for *LVEF* evaluated by cardiac magnetic resonance imaging (MRI) showing significantly better results in the *HiCT* group compared with the other groups after transplantation. The upper and lower borders of the box represent the upper and lower quartiles, the middle horizontal line represents the median, and the upper and lower whiskers represent the maximum and minimum values. \**P* < .05 versus sham; †*P* < .05 versus *HiCT*, Wilcoxon/Kruskal–Wallis test, post hoc Steel–Dwass multiple-comparison test. Four-week observation: sham, *n* = 7; *GHM*(–), *n* = 6; *HiCT*, *n* = 6; 12-week observation: sham, *n* = 7; *GHM*(–), *n* = 5; *HiCT*, *n* = 5. F, Representative cardiac MRI images at 4 weeks after surgery. *MI*, Myocardial infarction; *TX*, transplantation.



TABLE 1. Echocardiography data after treatment

Parameter	Pre-MI	Pretransplantation	1 wk	2 wk	4 wk	12 wk
LVDd, mm						
Sham	6.0 ± 0.3	8.1 ± 0.7	8.1 ± 0.8*	8.5 ± 0.5†	8.8 ± 0.5†	9.0 ± 0.4*
GHM(-)	5.6 ± 0.3	7.9 ± 0.3	8.0 (7.6-8.3)‡	7.9 ± 0.5§	8.4 ± 0.5	8.4 ± 0.3§
HiCT	5.7 ± 0.4	8.1 (7.9-8.2)	7.2 ± 0.3	7.1 ± 0.3	7.3 ± 0.6	7.3 ± 0.2
LVEDV, mL						
Sham	0.5 (0.4-0.6)	1.1 ± 0.3	1.2 ± 0.3¶	1.3 ± 0.2†	1.4 ± 0.2†	1.6 ± 0.2*
GHM(-)	0.4 ± 0.1	1.1 ± 0.1	1.1 ± 0.2‡	1.1 ± 0.2§	1.3 ± 0.2	1.3 ± 0.1§
HiCT	0.4 ± 0.1	1.1 (1.1-1.2)	0.8 ± 0.1	0.8 ± 0.1	0.9 ± 0.2	0.9 ± 0.1
LVEF, %						
Sham	92.7 ± 1.0	57.9 ± 5.0	59.0 ± 6.8†	55.6 ± 1.6†	56.1 ± 4.9†	57.5 ± 1.0*
GHM(-)	93.3 ± 1.3	56.8 ± 3.5	62.2 ± 4.7	62.2 ± 5.9	58.2 ± 8.0	67.4 ± 1.5§
HiCT	92.6 ± 1.5	56.9 ± 2.1	75.7 ± 5.6	75.7 ± 4.8	78.2 ± 5.1	82.7 ± 2.1
FS, %						
Sham	60.1 ± 1.8	26.9 ± 3.0	26.2 (24.9-30.1)†	25.6 ± 1.0†	25.9 ± 3.0†	26.7 ± 0.6*
GHM(-)	61.2 ± 2.6	26.1 ± 2.1	29.6 ± 3.0	29.7 ± 3.9	27.3 ± 4.9	33.2 ± 1.1§
HiCT	59.9 ± 2.9	26.2 ± 1.3	39.9 ± 5.2	39.8 ± 4.4	42.3 ± 5.3	46.5 ± 2.3

Four-week observation: sham, n = 18; GHM(-), n = 12; HiCT, n = 12; 12-week observation: sham, n = 8; GHM(-), n = 6; HiCT, n = 5. MI, Myocardial infarction; LVDd, left ventricular end-diastolic dimension; GHM(-), gelatin hydrogel microsphere negative; HiCT, human induced pluripotent stem cell-derived cardiac tissue; LVEDV, left ventricular end-diastolic volume; LVEF, left ventricular ejection fraction; FS, fractional shortening. \* $P < .05$  versus sham. † $P < .0001$  versus sham. ‡ $P < .01$  versus GHM(-). § $P < .05$  versus GHM(-). || $P < .001$  versus GHM(-); for all, the Wilcoxon/Kruskal-Wallis test and post hoc Steel-Dwass multiple-comparison test. ¶ $P < .01$  versus sham.

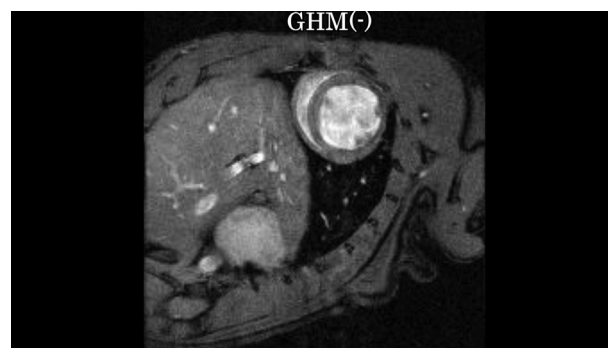
HiCT group compared with the other groups [sham vs GHM(-) vs HiCT: LVDd, 8.8 ± 0.5 mm vs 8.4 ± 0.5 mm vs 7.3 ± 0.6 mm,  $P < .0001$ ; LVEDV, 1.4 ± 0.2 mL vs 1.3 ± 0.2 mL vs 0.9 ± 0.2 mL,  $P < .0001$ ; LVEF, 56.1 ± 4.9% vs 58.2 ± 8.0% vs 78.2 ± 5.1%,  $P < .0001$ ; LV FS, 25.9 ± 3.0% vs 27.3 ± 4.9% vs 42.3 ± 5.3%,  $P < .0001$ ]. There were no significant differences in these parameters between the sham and GHM(-) groups. Echocardiography at 12 weeks post-transplantation revealed sustained functional recovery and prevention of LV dilatation [sham vs GHM(-) vs HiCT: LVDd, 9.0 ± 0.4 mm vs 8.4 ± 0.3 mm vs 7.3 ± 0.2 mm,  $P = .0001$ ; LVEDV, 1.6 ± 0.2 mL vs 1.3 ± 0.1 mL vs 0.9 ± 0.1 mL,  $P = .0009$ ; LVEF, 57.5 ± 1.0% vs 67.4 ± 1.5% vs 82.7 ± 2.1%,  $P = .0004$ ; LV FS, 26.7 ± 0.6% vs 33.2 ± 1.1% vs 46.5 ± 2.3%,  $P = .0004$ ] (Figure 2, A-D; Table 1).

Cardiac MRI at 4 and 12 weeks after transplantation showed the highest LVEF in the HiCT group compared with the other groups [sham vs GHM(-) vs HiCT: at 4 weeks, 38.1 ± 5.4% vs 43.8 ± 3.4% vs 54.0 ± 6.9%,  $P = .002$ ; at 12 weeks, 41.4 ± 4.2% vs 43.4% (IQR, 43.0%-46.5%) vs 54.1 ± 3.0%,  $P = .003$ ], consistent with the results of echocardiography (Figure 2, E and F; Video 2).

### Engraftment of HiCTs and Vascular Network Formation After Transplantation

We next histologically evaluated the transplanted grafts. All surviving rats during the observation period

were free from tumor formation both macroscopically and histologically. We measured the engraftment area by positive area of Ku80 immunostaining, a marker for human cells. At 4 weeks and 12 weeks after transplantation, the HiCT group showed a significantly larger median engraftment area compared with the GHM(-) group [GHM(-) vs HiCT, 4 weeks: 0.4 (IQR, 0.2-0.7) mm<sup>2</sup> vs 2.2 (IQR, 1.8-3.1) mm<sup>2</sup>;  $P = .005$ ; 12 weeks: 0 (IQR, 0-0.2) mm<sup>2</sup> vs 1.9 (IQR, 0.1-3.2) mm<sup>2</sup>,  $P = .026$ ] (Figure 3, A and B). Immunofluorescence staining images showed that von Willebrand factor (vWF)<sup>+</sup> ECs formed vascular networks among the engrafted cTnT<sup>+</sup> CMs



VIDEO 2. Representative cardiac magnetic resonance imaging movies at 4 weeks after surgery. Video available at: [https://www.jtcvs.org/article/S2666-2736\(21\)00340-5/fulltext](https://www.jtcvs.org/article/S2666-2736(21)00340-5/fulltext).

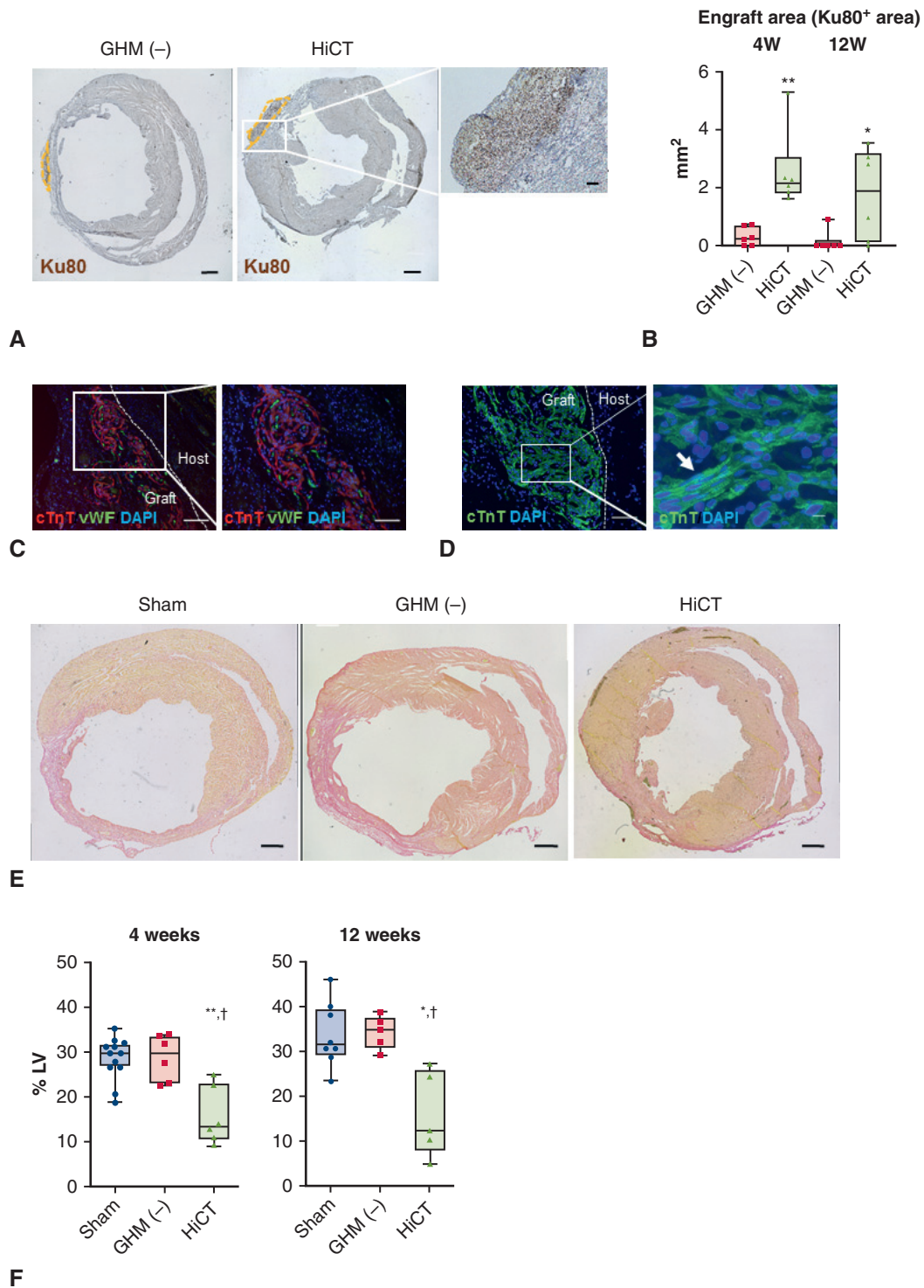


**FIGURE 3.** Engraftment and attenuation of ventricular remodeling after human induced pluripotent stem cell–derived cardiac tissue (*HiCT*) transplantation. A, Representative immunostaining for Ku80 (brown) at 4 weeks after surgery. *Left and center panels*, lower-magnification views. The *yellow dotted lines* indicate Ku80<sup>+</sup> area. (Scale bars: 1000  $\mu$ m.) *Right panel*, higher-magnification view. (Scale bar: 100  $\mu$ m.) B, Quantitative evaluation of the Ku80<sup>+</sup> area. The *HiCT* group showed a significantly larger engraftment area compared with the gelatin hydrogel microsphere–negative [*GHM*(-)] group in both study periods. The *upper and lower borders* of the box represent the upper and lower quartiles, the *middle horizontal line* represents the median, and the *upper and lower whiskers* represent the maximum and minimum values. \* $P < .05$ , \*\* $P < .01$ , Wilcoxon/Kruskal–Wallis test. Four-week observation: *GHM*(-),  $n = 6$ ; *HiCT*,  $n = 6$ ; 12-week observation: *GHM*(-),  $n = 6$ ; *HiCT*,  $n = 6$ . C and D, Representative immunofluorescence staining at engrafted graft regions. The *white*

(Figure 3, C). Furthermore, some engrafted CMs exhibited obvious striated sarcomeric structures, indicating structural maturation of CMs (Figure 3, D).

### Attenuation of LV Remodeling Mediated by HiCT Transplantation

The HiCT group exhibited significantly smaller scar areas by Sirius red staining (%LV) compared with other groups [sham vs GHM(-) vs HiCT, 4 weeks:  $28.5 \pm 4.8\%$  vs  $28.9 \pm 5.2\%$  vs  $15.8 \pm 6.5\%$ ;  $P = .006$ ; 12 weeks:  $33.8 \pm 7.3\%$  vs  $34.4 \pm 3.8\%$  vs  $16.7 \pm 8.9\%$ ,  $P = .005$ ] (Figure 3, E and F), indicating that functional recovery after HiCT transplantation was mediated by the attenuation of LV remodeling by virtue of the HiCT transplantation.

### Neovascularization After HiCT Transplantation and Vascular Network Formation in Engrafted HiCT

We evaluated the vascular density of the MI border zone and found that HiCT transplantation significantly increased the number of vWF<sup>+</sup> capillaries in close proximity to the graft compared with the sham and GHM(-) groups at 4 and 12 weeks after transplantation [sham vs GHM(-) vs HiCT, 4 weeks:  $2.5 \pm 0.8 \text{ mm}^2$  vs  $4.5 \pm 0.3 \text{ mm}^2$  vs  $9.6 \pm 1.1 \text{ mm}^2$ ,  $P = .0008$ ; 12 weeks:  $2.1 \pm 1.2 \text{ mm}^2$  vs  $2.9 \pm 0.6 \text{ mm}^2$  vs  $7.6 \pm 1.6/\text{mm}^2$ ,  $P = .006$ ] (Figure 4, A and B)

LSFM analysis revealed that although vascular structure in the grafts was not clearly observed at 3 days post-transplantation, marked vascular network formation in the grafts was observed at 2 weeks post-transplantation (Figure 4, C; Video 3). Histologic evaluation of vascular structures in the grafts at 12 weeks post-transplantation revealed that the vascular structure consisted of both human cells (Ku80<sup>+</sup>) and nonhuman rat cells (Ku80<sup>-</sup>/hematoxylin<sup>+</sup>), indicating that the formation of chimeric vascular networks originated from both hosts and grafts (Figure 4, D).

## DISCUSSION

In this study, we validated the efficacy of the inhibition of canonical Wnt/ $\beta$ -catenin signaling pathway in the differentiation of clinical-grade hiPSCs into cardiovascular

lineage cells. The transplantation of HiCTs onto a rat MI model exhibited greater cell survival and recovery of cardiac function in accordance with attenuated LV remodeling, possibly mediated by neovascularization (Figure 5). This work provides evidence supporting the possible clinical use of iPSCs in cardiovascular medicine and cardiac regenerative therapy, as originally established by Shinya Yamanaka.<sup>23</sup>

We first attempted to further improve our previously reported cell differentiation method<sup>16</sup> with modifications in which we evaluated the effect of inhibiting the canonical Wnt/ $\beta$ -catenin signaling pathway at the mesoderm stage of differentiation, which is reported to promote cardiac cell differentiation from pluripotent stem cells.<sup>24-26</sup> The Wnt/ $\beta$ -catenin signaling pathway is involved in a multitude of developmental processes and the maintenance of adult tissue homeostasis, including cell differentiation, proliferation, organogenesis, tissue regeneration, and tumorigenesis.<sup>25</sup> Although up-regulation of the Wnt/ $\beta$ -catenin signal is required for mesoderm differentiation, the cardiac specification process requires its inhibition, indicating the biphasic effect of the Wnt/ $\beta$ -catenin signal.<sup>24</sup> In the canonical Wnt/ $\beta$ -catenin signaling cascade, XAV939 inhibits tankyrase activity and increases the protein levels of the axin-GSK3 $\beta$  complex, which promotes  $\beta$ -catenin degradation by stabilizing axin.<sup>27</sup> IWP4 prevents palmitoylation of Wnt proteins, which inhibits Wnt production.<sup>25</sup> Administering these inhibitors of the Wnt/ $\beta$ -catenin signaling cascade during the cardiac specification process in our protocol at differentiation day 5 to 7 (mesoderm state) effectively increased CM (by 1.5-fold) and EC (by 1.4-fold) components. The validation of enhanced cardiovascular cell differentiation from clinical-grade hiPSCs through time-dependent regulation of canonical Wnt/ $\beta$ -catenin signal activity would be advantageous in promoting cardiac regenerative medicine based on hiPSCs. This is our first report of an effective modification of the method of induction of clinical-grade human iPS cell lines prepared for actual clinical use.

To further promote stem cell therapy, a suitable transplantation format that enables efficient cell engraftment is indispensable, considering the relatively poor efficiency of engraftment after transcatheter infusion or direct cell

← dotted line indicates the boundary of the host and graft tissues. C, Cardiac isoform of troponin-T (*cTnT*) (red; cardiomyocytes [CMs]), von Willebrand factor (vWF) (green; endothelial cells [ECs]) and 4',6-diamidino-2-phenylindole (DAPI) (blue; cell nuclei). (Scale bars: 200  $\mu\text{m}$  [left]; 100  $\mu\text{m}$  [right]). D, cTnT (green; CMs) and DAPI (blue; cell nuclei). The white arrow indicates sarcomeric structure. (Scale bars: 100  $\mu\text{m}$  in the left panel; 10  $\mu\text{m}$  in the right panel.) E, Representative Sirius Red staining at 4 weeks after surgery. (Scale bars: 1000  $\mu\text{m}$ .) F, Quantitative evaluations of scar area (%left ventricle [LV]). The HiCT group exhibited a significantly smaller scar area compared with the other groups. The upper and lower borders of the box represent the upper and lower quartiles, the middle horizontal line represents the median, and the upper and lower whiskers represent the maximum and minimum values. \* $P < .05$ , \*\* $P < .01$  versus sham, <sup>†</sup> $P < .05$  versus GHM(-), Wilcoxon/Kruskal-Wallis test, post hoc Steel-Dwass multiple-comparisons test. Four-week observation: sham,  $n = 11$ ; GHM(-),  $n = 6$ ; HiCT,  $n = 6$ ; 12-week observation: sham,  $n = 8$ ; GHM(-),  $n = 5$ ; HiCT,  $n = 6$ .



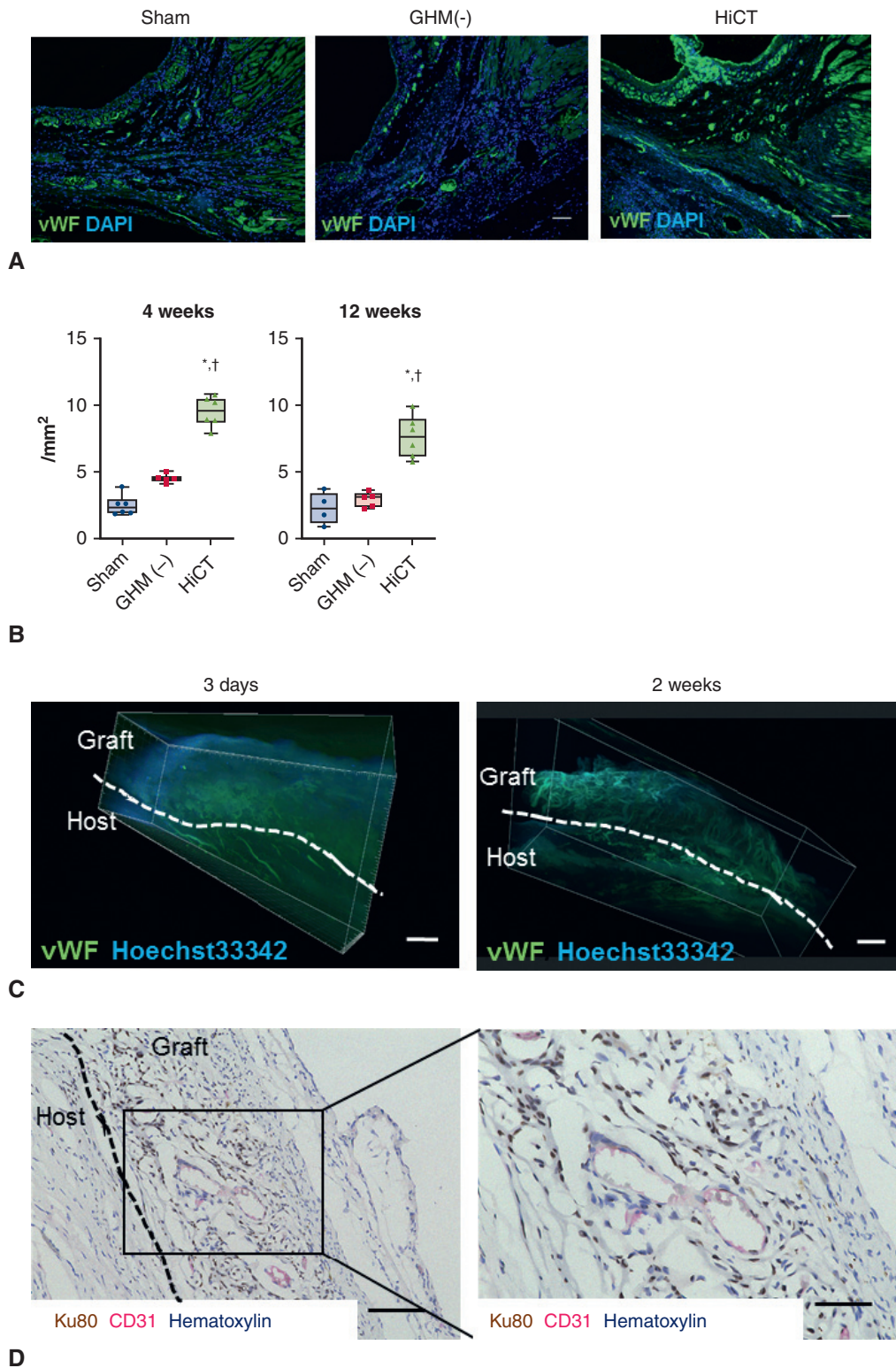
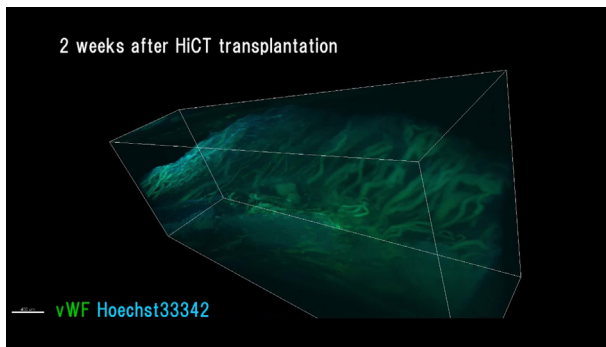


**FIGURE 4.** Neovascularization after human induced pluripotent stem cell–derived cardiac tissue (*HiCT*) transplantation. **A**, Representative immunofluorescence staining for von Willebrand factor (*vWF*) (green; endothelial cells [ECs]) and 4',6-diamidino-2-phenylindole (*DAPI*) (blue; cell nuclei) at the border zone of MI at 4 weeks after surgery. (Scale bars: 100  $\mu\text{m}$ .) **B**, Quantitative evaluation of vascular density ( $/\text{mm}^2$ ) at 4 and 12 weeks after surgery. *HiCT* transplantation significantly increased *vWF*<sup>+</sup> capillaries in close proximity to the graft compared with the sham and gelatin hydrogel microsphere–negative [*GHM*(-)] groups in both study periods. The *upper and lower borders* of the box represent the upper and lower quartiles, the *middle*



**VIDEO 3.** Representative light sheet fluorescence microscopy 3-dimensional movies at 3 days and 2 weeks after transplantation of clinical-grade human induced pluripotent stem cell-derived cardiac tissues. Video available at: [https://www.jtcvs.org/article/S2666-2736\(21\)00340-5/fulltext](https://www.jtcvs.org/article/S2666-2736(21)00340-5/fulltext).

injection into the myocardium owing to mechanical loss and the low survival rate of transplanted cells.<sup>28,29</sup> There is a known limitation of layering cell sheets to deliver a larger number of cells *in vivo*, as layering more than 3 cell sheets (>80  $\mu\text{m}$  thickness) does not provide a thicker construct because of hypoxic cell damage inside of the construct, leading to central necrosis.<sup>30</sup> To overcome the problem associated with cell sheet layering, we have established a bioengineered technology to enhance the viability of thick-layered mouse ESC-derived cardiac tissue sheets (>1 mm; 15 layers) using GHMs,<sup>19,20</sup> a biomaterial supporting oxygen and nutrient supply, which attenuates hypoxic cell death and apoptosis *in vitro* and augments engrafted volume and period *in vivo*.<sup>15</sup> In this study, we demonstrate that the application of GHMs with the layering of clinical-grade HiCTs boosts the temporospatial potential of engraftment of human tissue in rat hearts, as well as functional recovery by virtue of the enhanced engraftment (Figure 6).

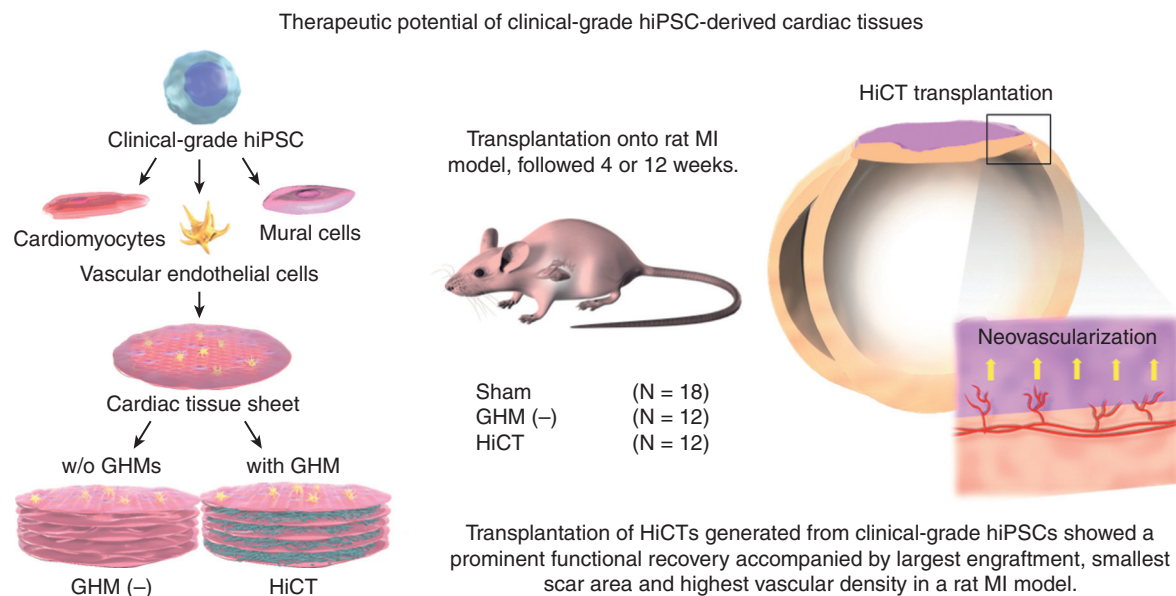
Histologic evaluation revealed that HiCT transplantation attenuated LV remodeling, which is commonly mediated by paracrine effects, such as neovascularization.<sup>16,31</sup> Tachibana and colleagues<sup>32</sup> reported that iPSC-derived CM transplantation conferred functional recovery in a mouse MI

model with paracrine effects mediated by various cytokines with antiapoptosis, proangiogenesis, or pro-cell migration effects. We previously reported that VEGF serves mainly as an angiogenic paracrine factor in mouse ESC-derived cardiac tissue sheet transplantation.<sup>16</sup> The therapeutic effect in this study might be attributed to the augmentation of anti-remodeling, angiogenic paracrine effects mediated by the engrafted tissue.

HiCT transplantation exhibited greater and longer engraftment of transplanted cells compared with GHM(-) transplantation. The engrafted tissue was supported by a vascular network consisting of chimeric vasculature with human and nonhuman vascular cells, which would have contributed to longer survival of the engrafted tissue. Although this requires further investigation, we presume that the engrafted tissue served as a “biological drug reservoir” that can provide preferential cytokines for the repair of damaged heart tissue through the circulatory connection between host and graft, and the therapeutic effects as a “reservoir” sustained by the longer survival of the engrafted tissue with a vascular network. The survival of transplanted grafts depends on an adequate nutrient and oxygen supply, which would be provided by direct diffusion from the surrounding tissue until the vascular network is formed. It may be possible that transplanted cardiac tissues supplemented with GHMs could survive only by direct diffusion until the development of tissue-equipped vascular networks that allow the long-term engraftment of HiCTs.

In this study, we validated the therapeutic potential of HiCTs using clinical-grade materials. The preclinical proof-of-concept of therapeutic efficacy with clinical-grade products has great significance for the realization of cardiac regenerative medicine using hiPSCs. We also need to recognize the areas remaining to be resolved for the clinical application of this strategy, including investigations of tumorigenicity<sup>8,33</sup> and arrhythmogenicity.<sup>34</sup> In particular, the risk of tumorigenicity should be studied before clinical implementation of this cell-based therapy. At least in the present study with its 4- and 12-week observation periods, we did not detect any neoplasm formation. In general, activation of the Wnt signaling pathway may be related to cancer formation owing to accelerated cell proliferation, according to previous

horizontal line represents the median, and the upper and lower whiskers represent the maximum and minimum values. \* $P < .05$  versus sham, <sup>†</sup> $P < .05$  versus GHM(-), Wilcoxon/Kruskal–Wallis test, post hoc Steel–Dwass multiple-comparison test. Four-week observation: sham,  $n = 6$ ; GHM(-),  $n = 5$ ; HiCT,  $n = 6$ ; 12-week observation: sham,  $n = 4$ ; GHM(-),  $n = 5$ ; HiCT,  $n = 6$ . C, Representative light sheet fluorescence microscopy (LSFM) image after 3 days (left) and 2 weeks (right) of HiCT transplantation. Hoechst 33342 staining (blue) indicates transplanted grafts. vWF (green) indicates the vascular structure. The white dotted line indicates the boundary of the host and graft tissues. Marked vascular network formation among the grafts was observed at 2 weeks after transplantation. (Scale bars: 700  $\mu\text{m}$  [left], 500  $\mu\text{m}$  [right]). D, Representative immunohistochemical image at 12 weeks after HiCT transplantation. The black dotted line indicates the boundary of host and graft tissues. Vascular structures among engrafted HiCT include both human (Ku80<sup>+</sup>) and nonhuman, rat cells (Ku80<sup>-</sup>, hematoxylin<sup>+</sup>). (Scale bars: 100  $\mu\text{m}$  [left], 50  $\mu\text{m}$  [right]). MI, Myocardial infarction.



hiPSC; human induced pluripotent stem cell, GHMs; gelatin hydrogel microspheres, HiCT: hiPSC derived cardiac tissue, MI; myocardial infarction

**FIGURE 5.** Transplantation of human induced pluripotent stem cell–derived cardiac tissue (*HiCT*) generated from clinical-grade human induced pluripotent stem cells (*hiPSCs*) showed prominent functional recovery accompanied by a smaller scar area and higher vascular density in a rat myocardial infarction model. *MI*, Myocardial infarction; *GHMs*, gelatin hydrogel microspheres.

studies.<sup>25</sup> On the other hand, we performed Wnt inhibition (not activation) in the present study, which might explain why we did not observe tumor formation. Nonetheless, we recognize the importance of further investigations of tumorigenicity with longer observation periods. In addition, further validation of therapeutic effects and mechanisms is needed in more severe pathologic conditions such as chronic ischemic cardiomyopathy and idiopathic dilated cardiomyopathy, the main disorders associated with heart transplantation and regenerative therapy. This, along with further refinements in the manufacturing and quality control of clinical-grade products, could provide a fundamental technological basis for hiPSC-based cardiac regenerative therapy as a standard therapeutic option in the future.

This study has several limitations. First, there is an interspecies difference between rats and humans, which raises the possibility that the immune reaction in rats might not be relevant to that in humans. To avoid interspecies bias, allogeneic transplantation experiments will be indispensable in our future studies.<sup>34,35</sup> Second, because MI in this study model was not atherosclerotic as in human clinical settings, but rather was induced by experimental coronary ligation, some of the biological effects of HiCT transplantation in our rat MI model might be inconsistent with those in human treatment. This possibility should

be evaluated using such medical modalities as myocardial perfusion scintigraphy in clinical trials.

## CONCLUSIONS

HiCT generated from clinical-grade hiPSCs is a feasible cell product for treating MI, as validated by our rat MI model experiments. Clinical-grade hiPSCs are a potentially reasonable cell source for cardiac regenerative medicine with foreseeable clinical applications.

## Conflict of Interest Statement

Dr Yamashita is a founder, equity holder, and scientific adviser of iHeart Japan Corporation. Drs Yamashita and Masumoto are co-inventors listed on multiple pluripotent stem cell–related patents. All other authors reported no conflicts of interest.

The *Journal* policy requires editors and reviewers to disclose conflicts of interest and to decline handling or reviewing manuscripts for which they may have a conflict of interest. The editors and reviewers of this article have no conflicts of interest.

We thank Kenji Kakuta (iHeart Japan Corp) for providing the clinical-grade HiCT; Yasuyo Matsubara and Naoko Tada (Kyoto University) for technical assistance with histology; Drs Hirohiko Imai and Tetsuya Matsuda (Kyoto University) for technical



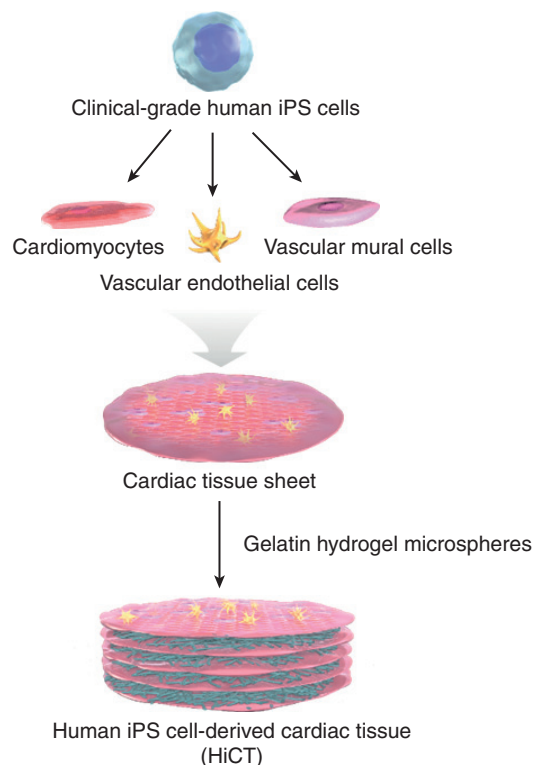


**FIGURE 6.** Human induced pluripotent stem cell-derived cardiac tissue (HiCT) generated from clinical-grade human induced pluripotent stem cells (hiPSCs) showed prominent therapeutic potential. Clinical-grade hiPSC lines established from a healthy volunteer were simultaneously differentiated into cardiovascular cell lineages. We seeded the cells on temperature-responsive culture dishes to form cell sheets. HiCTs were generated by stacking 5 cell sheets with gelatin hydrogel microspheres (GHMs) inserted between each sheet to promote oxygen and nutrition supply for the transplantation study. *iPS*, Induced pluripotent stem.

assistance with cardiac MRI; and Kanako Takakura, Dr Kenta Terai, and Dr Michiyuki Matsuda (Kyoto University) for technical assistance with LSM. We thank the Center for Anatomical, Pathological and Forensic Medical Research, Kyoto University Graduate School of Medicine for preparing microscope slides.

## References

- Mathur A, Arnold R, Assmus B, Bartunek J, Belmans A, Böning H, et al. The effect of intracoronary infusion of bone marrow-derived mononuclear cells on all-cause mortality in acute myocardial infarction: rationale and design of the BAMI trial. *Eur J Heart Fail.* 2017;19:1545-50.
- Ramireddy A, Brodt CR, Mendizabal AM, DiFede DL, Healy C, Goyal V, et al. Effects of transcatheter stem cell injection on ventricular proarrhythmia in patients with ischemic cardiomyopathy: results from the POSEIDON and TAC-HFT trials. *Stem Cells Transl Med.* 2017;6:1366-72.
- Miyagawa S, Domae K, Yoshikawa Y, Fukushima S, Nakamura T, Saito A, et al. Phase I clinical trial of autologous stem cell-sheet transplantation therapy for treating cardiomyopathy. *J Am Heart Assoc.* 2017;6:e003918.
- Takahashi K, Tanabe K, Ohnuki M, Narita M, Ichisaka T, Tomoda K, et al. Induction of pluripotent stem cells from adult human fibroblasts by defined factors. *Cell.* 2007;131:861-72.
- Colvin M, Smith JM, Hadley N, Skeans MA, Uccellini K, Goff R, et al. OPTN/SRTR 2018 annual data report: heart. *Am J Transplant.* 2020;20(Suppl s1):340-426.
- Cowger JA. Addressing the growing U.S. donor heart shortage: waiting for Godot or a transplant? *J Am Coll Cardiol.* 2017;69:1715-7.
- Li C, Chen S, Zhou Y, Zhao Y, Liu P, Cai J. Application of induced pluripotent stem cell transplants: autologous or allogeneic? *Life Sci.* 2018;212:145-9.
- Yamanaka S. Pluripotent stem cell-based cell therapy—promise and challenges. *Cell Stem Cell.* 2020;27:523-31.
- Doi D, Magotani H, Kikuchi T, Ikeda M, Hiramatsu S, Yoshida K, et al. Pre-clinical study of induced pluripotent stem cell-derived dopaminergic progenitor cells for Parkinson's disease. *Nat Commun.* 2020;11:3369.
- Taylor CJ, Peacock S, Chaudhry AN, Bradley JA, Bolton EM. Generating an iPSC bank for HLA-matched tissue transplantation based on known donor and recipient HLA types. *Cell Stem Cell.* 2012;11:147-52.
- Turner M, Leslie S, Martin NG, Peschanski M, Rao M, Taylor CJ, et al. Toward the development of a global induced pluripotent stem cell library. *Cell Stem Cell.* 2013;13:382-4.
- Narazaki G, Uosaki H, Teranishi M, Okita K, Kim B, Matsuoka S, et al. Directed and systematic differentiation of cardiovascular cells from mouse induced pluripotent stem cells. *Circulation.* 2008;118:498-506.
- Yamashita J, Itoh H, Hirashima M, Ogawa M, Nishikawa S, Yurugi T, et al. Flk1-positive cells derived from embryonic stem cells serve as vascular progenitors. *Nature.* 2000;408:92-6.
- Masumoto H, Matsuo T, Yamamizu K, Uosaki H, Narazaki G, Katayama S, et al. Pluripotent stem cell-engineered cell sheets reassembled with defined cardiovascular populations ameliorate reduction in infarct heart function through cardiomyocyte-mediated neovascularization. *Stem Cells.* 2012;30:1196-205.
- Matsuo T, Masumoto H, Tajima S, Ikuno T, Katayama S, Minakata K, et al. Efficient long-term survival of cell grafts after myocardial infarction with thick viable cardiac tissue entirely from pluripotent stem cells. *Sci Rep.* 2015;5:16842.
- Masumoto H, Ikuno T, Takeda M, Fukushima H, Marui A, Katayama S, et al. Human iPSC cell-engineered cardiac tissue sheets with cardiomyocytes and vascular cells for cardiac regeneration. *Sci Rep.* 2014;4:6716.
- Masumoto H, Nakane T, Tinney JP, Yuan F, Ye F, Kowalski WJ, et al. The myocardial regenerative potential of three-dimensional engineered cardiac tissues composed of multiple human iPSC cell-derived cardiovascular cell lineages. *Sci Rep.* 2016;6:29933.
- Ishigami M, Masumoto H, Ikuno T, Aoki T, Kawatou M, Minakata K, et al. Human iPSC cell-derived cardiac tissue sheets for functional restoration of infarcted porcine hearts. *PLoS One.* 2018;13:e0201650.
- Hayashi K, Tabata Y. Preparation of stem cell aggregates with gelatin microspheres to enhance biological functions. *Acta Biomater.* 2011;7:2797-803.
- Tabata Y. Tissue regeneration based on growth factor release. *Tissue Eng.* 2003;9(Suppl 1):S5-15.
- Susaki EA, Tainaka K, Perrin D, Kishino F, Tawara T, Watanabe TM, et al. Whole-brain imaging with single-cell resolution using chemical cocktails and computational analysis. *Cell.* 2014;157:726-39.
- Tainaka K, Kubota SI, Suyama TQ, Susaki EA, Perrin D, Ukai-Tadenuma M, et al. Whole-body imaging with single-cell resolution by tissue decolorization. *Cell.* 2014;159:911-24.
- Takahashi K, Yamanaka S. Induction of pluripotent stem cells from mouse embryonic and adult fibroblast cultures by defined factors. *Cell.* 2006;126:663-76.
- Naito AT, Shiojima I, Akazawa H, Hidaka K, Morisaki T, Kikuchi A, et al. Developmental stage-specific biphasic roles of Wnt/beta-catenin signaling in cardiomyogenesis and hematopoiesis. *Proc Natl Acad Sci U S A.* 2006;103:19812-7.
- Kahn M. Can we safely target the WNT pathway? *Nat Rev Drug Discov.* 2014;13:513-32.
- Fukushima H, Yoshioka M, Kawatou M, López-Dávila V, Takeda M, Kanda Y, et al. Specific induction and long-term maintenance of high purity ventricular cardiomyocytes from human induced pluripotent stem cells. *PLoS One.* 2020;15:e0241287.
- Huang SM, Mishina YM, Liu S, Cheung A, Stegmeier F, Michaud GA, et al. Tankyrase inhibition stabilizes axin and antagonizes Wnt signaling. *Nature.* 2009;461:614-20.
- Sekine H, Shimizu T, Dobashi I, Matsuura K, Hagiwara N, Takahashi M, et al. Cardiac cell sheet transplantation improves damaged heart function via superior cell survival in comparison with dissociated cell injection. *Tissue Eng Part A.* 2011;17:2973-80.



29. Pelacho B, Mazo M, Gavira JJ, Prósper F. Adult stem cells: from new cell sources to changes in methodology. *J Cardiovasc Transl Res.* 2011;4:154-60.
30. Shimizu T, Sekine H, Yang J, Isoi Y, Yamato M, Kikuchi A, et al. Polysurgery of cell sheet grafts overcomes diffusion limits to produce thick, vascularized myocardial tissues. *FASEB J.* 2006;20:708-10.
31. Kocher AA, Schuster MD, Szabolcs MJ, Takuma S, Burkhoff D, Wang J, et al. Neovascularization of ischemic myocardium by human bone-marrow-derived angioblasts prevents cardiomyocyte apoptosis, reduces remodeling and improves cardiac function. *Nat Med.* 2001;7:430-6.
32. Tachibana A, Santoso MR, Mahmoudi M, Shukla P, Wang L, Bennett M, et al. Paracrine effects of the pluripotent stem cell-derived cardiac myocytes salvage the injured myocardium. *Circ Res.* 2017;121:e22-36.
33. Lee AS, Tang C, Rao MS, Weissman IL, Wu JC. Tumorigenicity as a clinical hurdle for pluripotent stem cell therapies. *Nat Med.* 2013;19:998-1004.
34. Shiba Y, Gomibuchi T, Seto T, Wada Y, Ichimura H, Tanaka Y, et al. Allogeneic transplantation of iPS cell-derived cardiomyocytes regenerates primate hearts. *Nature.* 2016;538:388-91.
35. Kawamura T, Miyagawa S, Fukushima S, Maeda A, Kashiwayama N, Kawamura A, et al. Cardiomyocytes derived from MHC-homozygous induced pluripotent stem cells exhibit reduced allogeneic immunogenicity in MHC-matched non-human primates. *Stem Cell Reports.* 2016;6:312-20.

**Key Words:** induced pluripotent stem cell, cardiac regenerative therapy, heart failure, transplantation

## APPENDIX 1. METHODS

### Differentiation of Clinical-Grade hiPSCs into Cardiovascular Cell Lineages

We used clinical-grade hiPSC lines (FfI01s04 and QHJI01s04) that are peripheral monocyte-derived HLA-homozygous hiPSCs established at the Facility for iPS Cell Therapy Center for iPS Cell Research and Application, Kyoto University. For cardiovascular cell differentiation, we dissociated hiPSCs using  $\times 0.5$  TrypLE Select (Thermo Fisher Scientific, Waltham, Mass) diluted with 0.5 mM EDTA and plated them onto Matrigel-coated plates (growth factor reduced, 1:60 dilution; Corning Inc, Corning, NY) at a density of approximately 150,000 to 160,000 cells/cm<sup>2</sup> in AK02N or AK03N medium (Ajinomoto Pharma, Tokyo, Japan) with 10  $\mu$ M Y-27632 (FUJIFILM Wako Pure Chemical, Osaka, Japan) 2 days before induction. Cells were covered with Matrigel (1:60 dilution) and AK02N or AK03N medium 1 day before induction. The medium was replaced with RPMI + B27 medium (RPMI 1640 plus 2 mM L-glutamine or Glutamax plus B27 supplement without insulin) (Thermo Fisher Scientific, Waltham, Mass) supplemented with 100 ng/mL Activin A (R&D Systems, Minneapolis, Minn) for 1 day, followed by 10 ng/mL bone morphogenetic protein 4 (BMP4; R&D Systems) and 10 ng/mL basic fibroblast growth factor (bFGF; FUJIFILM Wako Pure Chemical) for 4 days without culture medium change.

At differentiation day 5, the culture medium was replaced with RPMI + B27 medium with 50 ng/mL recombinant human vascular endothelial growth factor 165 amino-acid isoform (VEGF<sub>165</sub>; FUJIFILM Wako Pure Chemicals) and Wnt inhibitors (5  $\mu$ M XAV939 [Merck Millipore, Burlington, Mass] and 2.5  $\mu$ M IWP4 [Stemgent, Cambridge, Mass]). Culture medium was refreshed every other day with RPMI + B27 medium supplemented with 50 ng/mL VEGF<sub>165</sub>. All reagents were prepared with clinical-grade materials for the culture of QHJI01s04 iPS cells.

At 13 to 15 days after differentiation, cardiovascular cells were dissociated by incubation with Accumax (Innovative Cell Technologies, San Diego, Calif) or Versene (Thermo Fisher Scientific) plus 0.05% Trypsin solution with EDTA (Thermo Fisher Scientific) and seeded on fetal bovine serum (FBS)-coated 12-well temperature-responsive culture plates (UpCell; CellSeed, Tokyo, Japan)<sup>E1,E2</sup> with a cell density of  $1.5 \times 10^6$  cells/well with 3 mL of alpha minimum essential medium ( $\alpha$ MEM; Thermo Fisher Scientific) or RPMI 1640 supplemented with 10% FBS or B27, 50 to 100 ng/mL VEGF<sub>165</sub>, and 20  $\mu$ M Y-27632 or, alternatively, 5.5 mmol/L 2-mercaptoethanol, 50,000 U/L penicillin, and 50 mg/L streptomycin, at 37 °C under 5% CO<sub>2</sub>. At 2 to 4 days after seeding, the culture plates were moved to room temperature for detachment of cell sheets. Cell sheets detached spontaneously within 15 to 30 minutes.

### Preparation of HiCTs

Each detached cell sheet was gently aspirated into a 10-mL pipette and transferred onto a noncoated or Matrigel-coated 60-mm culture dish. Once the cell sheet was spread without folds by aspirating the medium, GHMs dissolved with 10  $\mu$ L of phosphate-buffered saline (50  $\mu$ g/ $\mu$ L) were spread on the surface of the cell sheet. The dishes were incubated at 37 °C for 45 minutes to allow the cell sheet to adhere to the culture dish. Then the second cell sheet was placed on the top of the first sheet and attached without folds by aspirating the media. Similarly, stacked constructs with 5 layers (HiCTs) were prepared. We also prepared 5 layers of stacked sheet without GHMs as GHM(-). Transplantation was performed 1 day after stacking. HiCTs and GHM(-) generated with GMP-grade materials were prepared and provided by iHeart Japan Corporation (Kyoto, Japan). GHMs were prepared by dehydrothermal cross-linking of gelatin microspheres prepared in a water in oil emulsion state according to a previously reported method.<sup>E1,E3</sup> GMP-grade GHMs were provided by Shibuya-Kogyo Industries (Kanazawa, Japan).

### Flow Cytometry Analysis

For flow cytometry analysis, differentiated cells were stained with combinations of allophycocyanin-conjugated CD90, phycoerythrin (PE)-conjugated PDGFR- $\beta$  (BD Biosciences, San Jose, Calif), PE-conjugated vascular endothelial cadherin (VE-cadherin), and PE-conjugated TRA-1-60 (BD Biosciences). Cells were stained with the LIVE/DEAD Fixable Aqua Dead Cell Staining Kit (Thermo Fisher Scientific) to eliminate dead cells. For intracellular proteins, cells were fixed with 4% paraformaldehyde (PFA) and stained with combinations of cardiac isoform of troponin T (cTnT; Thermo Fisher Scientific) labeled with Alexa Fluor 488 using Zenon technology (Thermo Fisher Scientific), then subjected to analysis with a FACS Aria II (BD Biosciences) and FACS-Diva software version 8.0 (BD Biosciences).

### Animals

Male athymic nude rats (F344/NJcl-rnu/rnu, 8-12 weeks old) were purchased from CLEA Japan (Tokyo, Japan) and housed in a controlled environment. All animal experimental protocols were approved by the Animal Experimentation Committee of Kyoto University (#Med Kyo 19540). All animal experiments were performed according to the Guidelines for Animal Experiments of Kyoto University, which conform to Japanese law and the US National Research Council's *Guide for the Care and Use of Laboratory Animals*.

### MI Induction and HiCT Transplantation

The animals were intubated with a 16-gauge angiocath (Terumo, Tokyo, Japan) and mechanically ventilated under

general anesthesia with 2% isoflurane (Pfizer, Tokyo, Japan). The heart was exposed by a left anterolateral thoracotomy. MI was induced by permanent ligation of the left anterior descending coronary artery as described previously.<sup>E1</sup> Rats with an LV FS of <30% by echocardiography on day 7 after ligation were enrolled in further experiments. Each enrolled rat was assigned at random to 1 of 3 groups: 4 weeks of observation and MI operation without transplantation (sham; n = 18), GHM(-) transplantation group (n = 12), or the HiCT transplantation group (n = 12). Parts of the 3 groups—sham, n = 8; GHM(-), n = 6; HiCT, n = 5—were followed until 12 weeks post-transplantation.

In this study, we performed left anterior descending artery ligation in a total of 89 rats. Nineteen rats (21%) experienced early death from MI, and 28 rats were excluded because of insufficient MI and other reasons; thus, 42 rats were enrolled in the experiments. One rat in the HiCT group died just before the 12-week echocardiography, and 1 rat in the GHM(-) group died just before the 12-week cardiac MRI from the anesthesia procedure.

Stacked cell sheets were transplanted onto the surface of the anterior wall of the heart as described previously.<sup>E1</sup> The sheets were spread manually to cover the entire MI area and border area and could be placed onto the surface of the heart without sutures. To prevent detachment of the cell sheets, we placed a sodium hyaluronate/carboxymethylcellulose absorbable barrier (Septrafilm; Kaken Pharmaceutical, Tokyo, Japan) on the graft. The chest was closed 15 to 20 minutes after surgery.

### Cardiac Function Analysis With Echocardiography and MRI

The evaluation of cardiac function, echocardiography was performed using the Vivid 7 system (GE Healthcare, Chicago, Ill) and an 11-MHz imaging transducer (10S ultrasound probe; GE Healthcare) before ligation (baseline; pre-MI), on the day of transplantation (7 days post-MI; pre-transplantation), and at 1, 2, 4, and 12 weeks after transplantation. LVDd, LVEDV, LVEF, and FS were recorded and measured using M-mode echocardiography and the Teichholz method. %FS was calculated as follows:  $FS = (LVDd - LVDs [LV \text{ end-systolic dimension}]) / LVDd$ .

In addition, at the end of the observation period for each group, under general anesthesia with 2% isoflurane (Pfizer), MRI (7-T BioSpec 70/20 USR; Bruker Biospin, Ettlingen, Germany) was used for another functional evaluation. LVEDV and LV end-systolic volume (LVESV) were obtained using ImageJ software, and LVEF was calculated using the following formula:  $LVEF (\%) = 100 \times (LVEDV - LVESV) / LVEDV$ .

### Histologic Analysis

HiCTs maintained in culture with 3 mL of  $\alpha$ MEM supplemented with 10% FBS, 5.5 mmol/L 2-mercaptoethanol,

50,000 U/L penicillin, 50 mg/L streptomycin, and 100 ng/mL VEGF<sub>165</sub> at 37 °C and under 5% CO<sub>2</sub> for 1 week (with medium changed every other day) were fixed in 4% PFA and embedded in paraffin. Then 5- $\mu$ m sections were obtained and stained with hematoxylin and eosin.

At the end of the observation period, animals were sacrificed. Heart tissue samples were fixed in 4% PFA, embedded in optimum cutting temperature compound (Sakura Finetek Japan, Tokyo, Japan), and frozen. Five 5- $\mu$ m-thick sections were obtained at 50- $\mu$ m intervals along the short axis from the ligation point of the left anterior descending artery for each rat and examined by Sirius Red (FUJIFILM Wako Pure Chemicals), and immunohistochemical and immunofluorescence staining of Ku80, CD31, cTnT, and vWF. For immunohistochemical staining to measure engraftment, sections were treated with Protein Block, Serum-Free (Agilent, Santa Clara, Calif) and incubated overnight with primary antibodies at 4 °C. A rabbit monoclonal anti-Ku80 antibody (Abcam, Cambridge, Mass; 1:500) and Histofine Simple Stain MAX PO (MULTI) (Nichirei Biosciences, Tokyo, Japan) was used for DAB staining. In addition, to evaluate human cells and vascular structure in engraft area, double staining with a rabbit polyclonal anti-Ku80 antibody (Cell Signaling Technology, Danvers, Mass; 1:200) and mouse monoclonal anti-CD31 antibody (Leica Biosystems, Buffalo Grove, Ill; 1:100) was conducted using a conventional ABC method (avidin-biotin-peroxidase complex, ABC-Elite; Vector Laboratories, Burlingame, Calif). For immunofluorescence imaging, a rabbit polyclonal anti-vWF antibody (Abcam; 1:3000) and a mouse monoclonal anti-cTnT antibody (Lab Vision Corporation, Fremont, Calif; 1:500) were used for double staining with vWF and cTnT. Anti-mouse Alexa Fluor 546 (Thermo Fisher Scientific; 1:400) and anti-rabbit Alexa Fluor 488 (Thermo Fisher Scientific; 1:400) were used as secondary antibodies. The area of engraftment was measured by manual trace of 5 sections of the Ku80-positive area for each rat. Scar area (% fibrosis area/total LV area, with Sirius Red staining) was manually traced and measured from 5 sections for each rat using ImageJ software.<sup>E4</sup> Histologic samples were photographed and analyzed using an all-in-one microscope (Biorevo BZ-X810; Keyence, Osaka, Japan).

### Tissue Clearing and LSFM for Vasculogenesis Analysis After Transplantation

At 3 days and 2 weeks after HiCT transplantation, we sacrificed some animals for preparation of tissue clearing samples. In this experiment, we treated cardiac tissue sheets with Hoechst 33342 before preparing HiCTs to detect engrafted tissues in vivo. Heart tissue was fixed in 4% PFA and subjected to a tissue-clearing reagent, CUBIC (clear, unobstructed brain imaging cocktails and computational

analysis sample).<sup>E5,E6</sup> To prepare the sample, the following reagents were applied sequentially: Tissue Clearing Reagent CUBIC-L (Tokyo Chemical Industry, Tokyo, Japan) for approximately 10 days in a 37 °C incubator, rabbit polyclonal anti-vWF antibody (Abcam; 1:3000) for 3 days, anti-rabbit Alexa Fluor 488 (Thermo Fisher Scientific; 1:400) for 3 days, and Tissue Clearing Reagent CUBIC-R (Tokyo Chemical Industry) for 1 day.

Images of cleared hearts were acquired using a Zeiss Lightsheet Z.1 microscope (Zeiss, Oberkochen, Germany) equipped with a single side light sheet and 2 pairs of lenses: an EC Plan-Neofluar 5 × /0.16 detection objective lens and an LSM clearing 5 × /0.1 illumination objective lens. The excitation wavelength for fluorescein isothiocyanate was 561 nm. Pre-installed laser-blocking filter (LBF 405/455/561/640), a secondary beam splitter (SBS LP510), and an emission filter (BP 420-470) were used.

Images were saved in the multilayer 16-bit tagged image file format. Zen software (Zeiss) was used to control the microscope and to acquire images. A 3D image of cleared tissue was reconstructed using Imaris 8.3.1 (Oxford Instruments, Abingdon, UK).

### Statistical Analysis

Nonnormally distributed data are presented as median (IQR), and normally distributed data are presented as

mean ± SD. All data analyses were performed using JMP Pro 15.1 (SAS Institute, Cary, NC). For comparisons between 2 groups, *P* values were obtained using the Wilcoxon/Kruskal–Wallis test. Comparisons between >2 groups were performed using the Wilcoxon/Kruskal–Wallis test, and post hoc comparisons were performed using the Steel–Dwass multiple-comparison test. *P* < .05 was considered statistically significant. All graphs were created using GraphPad Prism 8 J for Windows version 8.3.0 (GraphPad Software, San Diego, Calif).

### E-References

- E1. Matsuo T, Masumoto H, Tajima S, Ikuno T, Katayama S, Minakata K, et al. Efficient long-term survival of cell grafts after myocardial infarction with thick viable cardiac tissue entirely from pluripotent stem cells. *Sci Rep.* 2015;5:16842.
- E2. Masumoto H, Ikuno T, Takeda M, Fukushima H, Marui A, Katayama S, et al. Human iPS cell-engineered cardiac tissue sheets with cardiomyocytes and vascular cells for cardiac regeneration. *Sci Rep.* 2014;4:6716.
- E3. Hayashi K, Tabata Y. Preparation of stem cell aggregates with gelatin microspheres to enhance biological functions. *Acta Biomater.* 2011;7:2797-803.
- E4. Schneider CA, Rasband WS, Eliceiri KW. NIH Image to ImageJ: 25 years of image analysis. *Nat Methods.* 2012;9:671-5.
- E5. Susaki EA, Tainaka K, Perrin D, Kishino F, Tawara T, Watanabe TM, et al. Whole-brain imaging with single-cell resolution using chemical cocktails and computational analysis. *Cell.* 2014;157:726-39.
- E6. Tainaka K, Kubota SI, Suyama TQ, Susaki EA, Perrin D, Ukai-Tadenuma M, et al. Whole-body imaging with single-cell resolution by tissue decolorization. *Cell.* 2014;159:911-24.